

Polymeric Structures in Aluminium and Gallium Halides

Z. Akdeniz, M. Çaliskan^a, Z. Çiçek, and M. P. Tosi^b

Physics Department, University of Istanbul, Istanbul, Turkey

^a Department of Physics, Trakya University, Edirne, Turkey

^b INFN and Classe di Scienze, Scuola Normale Superiore, Pisa, Italy

Reprint requests to Prof. M. P. T.; Fax: +39-50-563513; E-mail: tosim@sns.it

Z. Naturforsch. **55 a**, 575–580 (2000); received February 18, 2000

The anionic species $(\text{Al}_n\text{X}_{3n+1})^-$ with $\text{X} = \text{Cl}$ or Br and $n \geq 1$ have been recognized for a number of years to form in acidic liquid mixtures of aluminium chloride or bromide with the corresponding halides of alkali or organic cations, in relative proportions which vary with the composition of the mixture. In this work we evaluate the structure and the energetics of such polymeric series in a comparative study of Al and Ga compounds. To this end we first extend an earlier study of the ionic interactions in the Al_2Cl_6 molecule [Z. Akdeniz and M. P. Tosi, Z. Naturforsch. **54a**, 180 (1999)] to determine microscopic ionic models for Ga_2Cl_6 , Al_2Br_6 , and Ga_2Br_6 . The models are then used (i) to evaluate the polymeric clusters for $n \leq 4$ in the two trivalent-metal chlorides, and (ii) to explore the potential-energy hypersurface of alkali counterions in the case $n = 2$. We present tests of the results against available data and an evaluation of the convergence of the energy of the polymeric series towards a value of about 0.5 eV per monomer.

Key words: Ionic Clusters; Molecular Vapours; Molten Salts.

1. Introduction

Liquid chloro- and bromo-aluminates, represented by the formula $(\text{AX})_{1-x} \cdot (\text{AlX}_3)_x$ where $\text{X} = \text{Cl}$ or Br and A denotes an alkali or an organic cation, have been studied extensively for a number of years (for a recent review see [1]). Main attention has been given to the acidic range of composition ($0.5 \leq x \leq 1$). Various evidence from several types of experiments and from molecular dynamics calculations shows that, starting from the mixture at $x = 0.5$ as a liquid of tetrahedral $(\text{AlX}_4)^-$ anions and A^+ counterions, polymeric species of the type $(\text{Al}_n\text{X}_{3n+1})^-$ with $n \geq 2$ are formed as the composition of the liquid mixture is varied towards pure AlX_3 . The pure compound forms a molecular liquid of Al_2X_6 dimers.

The available evidence has stimulated molecular-orbital studies by *ab initio* methods on the isolated $(\text{Al}_2\text{Cl}_7)^-$ complex anion [2] as well as by semi-empirical methods on the $(\text{Al}_2\text{X}_7)^-$ and $(\text{Al}_3\text{X}_{10})^-$ clusters [3–5]. It is known from these studies that the $(\text{Al}_2\text{X}_7)^-$ cluster is formed by two tetrahedra sharing a halogen corner [2–4] and that for the $(\text{Al}_3\text{X}_{10})^-$ species a chain-like structure of corner-sharing tetrahedra is more stable than a ring-like structure by 10

–15 kcal/mole [3]. A preliminary *ab initio* study of the effect of an alkali counterion on the chlorine bridge in $(\text{Al}_2\text{Cl}_7)^-$ has also been reported [3]. There remains an interest to study how a chain-like polymeric series of the $(\text{Al}_n\text{X}_{3n+1})^-$ type converges structurally and energetically with increasing n and to learn about the role of the chemical nature of the trivalent-metal ion, *e. g.* about the consequences of substituting the Al ions by Ga ions [6]. It also seems interesting to investigate the shape of the potential energy hypersurface for counterions around the anionic species.

In the present work we address the above questions by means of a microscopic ionic model. We start from an earlier study of the ionic interactions in Al_2Cl_6 -based clusters [7] and extend it in Sect. 2 to determine models of the interionic forces for Al and Ga chlorides and bromides from properties of the Ga_2Cl_6 , Al_2Br_6 , and Ga_2Br_6 molecular dimers. These models are then used in Sect. 3 to evaluate the structure and the energetics of polymeric anions with $n \leq 4$ for the two trivalent-metal chlorides, and in Sect. 4 to investigate the local potential-energy minima for alkali counterions around the $(\text{Al}_2\text{X}_7)^-$ and $(\text{Ga}_2\text{X}_7)^-$ clusters. We conclude the paper in Sect. 5 with a brief summary and discussion of our results.

0932-0784 / 00 / 0600-0575 \$ 06.00 © Verlag der Zeitschrift für Naturforschung, Tübingen · www.znaturforsch.com



Dieses Werk wurde im Jahr 2013 vom Verlag Zeitschrift für Naturforschung in Zusammenarbeit mit der Max-Planck-Gesellschaft zur Förderung der Wissenschaften e.V. digitalisiert und unter folgender Lizenz veröffentlicht: Creative Commons Namensnennung-Keine Bearbeitung 3.0 Deutschland Lizenz.

Zum 01.01.2015 ist eine Anpassung der Lizenzbedingungen (Entfall der Creative Commons Lizenzbedingung „Keine Bearbeitung“) beabsichtigt, um eine Nachnutzung auch im Rahmen zukünftiger wissenschaftlicher Nutzungsformen zu ermöglichen.

This work has been digitalized and published in 2013 by Verlag Zeitschrift für Naturforschung in cooperation with the Max Planck Society for the Advancement of Science under a Creative Commons Attribution-NoDerivs 3.0 Germany License.

On 01.01.2015 it is planned to change the License Conditions (the removal of the Creative Commons License condition “no derivative works”). This is to allow reuse in the area of future scientific usage.

Table 1. Interionic force parameters in Al and Ga chlorides and bromides (the subscripts M and X denote the trivalent-metal ion and the halogen ion; the values for Al_2Cl_6 are from [7]).

	z_M	z_X	R_M (Å)	ρ_M (Å)	R_X (Å)	ρ_X (Å)	C_X (eÅ ^{5/2})	α_X (Å ³)	α_s (Å ³ /e)
Al_2Cl_6	2.47 ₂	-0.82 ₄	0.95	0.044	1.71	0.238	5.5	2.05	0.46
Al_2Br_6	2.42 ₇	-0.80 ₉	0.95	0.044	1.84	0.258	7.2	3.05	0.76
Ga_2Cl_6	2.36 ₄	-0.78 ₈	0.97	0.045	1.71	0.238	5.5	2.05	0.46
Ga_2Br_6	2.36 ₄	-0.78 ₈	0.97	0.045	1.84	0.258	7.2	3.05	0.76

	M-X ^T	M-X ^B	M-M	X ^T -X ^T	X ^B -X ^B	∠X ^T -M-X ^T	∠X ^B -M-X ^B
Al_2Cl_6 : model	2.065	2.28	3.20	3.59	3.23	121	90
Al_2Br_6 : model	2.22	2.43	3.34	3.84	3.54	120	93
ED	2.22	2.41	3.34	3.90	3.48	122.8	92.3
QC	2.25	2.46	3.43	3.91	3.52	120.8	91.4
Ga_2Cl_6 : model	2.13	2.34	3.32	3.70	3.29	121	90
Ga_2Br_6 : model	2.27	2.48	3.43	3.93	3.59	120	93
ED	2.25	2.45	3.43	4.04	3.49	128.1	91.1
QC	2.29	2.50	3.52	4.00	3.56	122.1	90.7

Table 2. Equilibrium structure of Al_2Cl_6 , Al_2Br_6 , Ga_2Cl_6 and Ga_2Br_6 (bond lengths in Å and bond angles in degrees; the values for Al_2Cl_6 are from [7]).

2. Interionic Force Model

In an earlier study of Al_2Cl_6 and related aluminium chloride clusters including $(\text{Al}_2\text{Cl}_7)^-$ [7] two of us constructed an expression for the potential energy $U(\{\mathbf{r}_{ij}\}, \{\mathbf{p}_i\})$ of an ionic cluster as a function of the interionic bond vectors \mathbf{r}_{ij} and of the electric dipole moments \mathbf{p}_i . This involved an extension of the shell model (also known as the deformation dipole model) for the lattice dynamics of ionic and semiconducting crystals [8]. A basic quantal justification for this approach to molecular structure has been given for alkali halides by means of exchange perturbation theory [9, 10]. For the detailed expressions entering $U(\{\mathbf{r}_{ij}\}, \{\mathbf{p}_i\})$, which are also used in the present study, we refer to the earlier work [7].

In the determination of the model parameters for Al_2Br_6 we closely follow the procedure already developed in [7] for the Al_2Cl_6 dimer. We start from an earlier study of the $(\text{AlBr}_4)^-$ cluster [11] and refine it with special attention to the modelling of the bridge formed by two bromines in the dimer. This is done by introducing an effective valence z_{Br} for the bromine and polarizabilities α_{Br} and α_s , which describe dipole induction by the electric field on the halogen and its saturation by short-range overlap distortions of its electron shells. We determine these quantities for Al_2Br_6 from the measured value of its topmost stretching-mode frequency ($\nu_3 = 500 \text{ cm}^{-1}$ [12]) and from the Al-Al bond length (3.34 Å) and the Al-terminal bromine bond length (2.22 Å) as measured in an electron diffraction experiment [13]. The other model

parameters for the bromine ion (the van der Waals coefficient C_{Br} , the ionic radius R_{Br} , and the stiffness parameter ρ_{Br} describing the contribution of the bromines in the Busing form [14] of the Al-Br overlap repulsions) are taken from [11], while the ionic radius R_{Al} and the stiffness parameter ρ_{Al} for the Al ion are taken from [7]. Overall charge neutrality determines $z_{\text{Al}} = -3z_{\text{Br}}$.

The extension of these model parameters to the Ga dimers is immediate. We use as input data for Ga_2Br_6 the measured Ga-Ga bond length (3.43 Å) from electron diffraction experiments [13] and the measured value of the breathing mode of the molecular dimer in the pure molecular liquid ($\nu_b = 290 \text{ cm}^{-1}$ [15]) to determine the effective valence and the ionic radius of Ga, on the assumption that the other model parameters can be transferred from the Al_2Br_6 dimer. For Ga_2Cl_6 , on the other hand, transfer of all model parameters from Ga_2Br_6 and from Al_2Cl_6 yields immediate agreement with the rather scanty experimental evidence on the Raman frequencies of the dimer in the liquid as measured by Boghosian *et al.* [16]. In particular, we calculate a frequency of 411 cm^{-1} for the breathing mode against a measured value of 410 cm^{-1} [16].

Table 1 shows the sets of model parameters that we have used in the calculations reported in the sequel for the Al and Ga halide polymers. It is evident that all these materials are reasonably close to the ideal ionic model, as can be judged from the values of the effective valences. The deviations from ideal ionicity are slightly larger for bromides and for Ga compounds.

Table 3. Frequencies of vibrational modes for Al_2Br_6 and Ga_2Br_6 (in cm^{-1} ; values in curly brackets are estimated).

	— Al_2Br_6 —		— Ga_2Br_6 —	
	model	Expt. gas [12]	model	Expt. liquid [15]
B_{1u}	10	{8}	9	—
A_u	34	{30}	31	—
A_g	59	59	55	62
B_{3g}	59	{67}	56	—
B_{2g}	75	76	63	69
B_{2u}	80	90	71	—
B_{3u}	86	{110}	76	—
B_{1u}	104	112	84	84
B_{1g}	110	114	93	—
A_g	159	139	132	118
B_{3u}	170	199	133	—
B_{1g}	199	203	175	—
A_g	217	{250}	202	201
B_{2u}	355	346	239	—
B_{3u}	366	376	269	—
A_g	419	409	<u>290</u>	290
B_{2g}	492	489	333	341
B_{1u}	<u>500</u>	500	334	—

Table 2 completes the comparison of our results for the equilibrium structure of the molecular dimers with measured values from electron diffraction (ED, from [13]) and with the results of quantum chemical calculations (QC, from [15]). The symbols X^T and X^B denote a terminal and a bonding halogen, respectively. Values fitted to experiment are underlined.

Table 3 compares our results for the vibrational frequencies of Al_2Br_6 and Ga_2Br_6 with experimental data on gaseous Al_2Br_6 [12] and on the GaBr_3 molecular liquid [15], respectively. The agreement between calculated and measured spectra in Table 3 can be considered as very reasonable.

3. Equilibrium Structures and Energetics of the Polymeric Series

As already discussed in earlier work (see *e. g.* [7]), the potential energy landscape for the $(\text{Al}_2\text{Cl}_7)^-$ anion is very complex. Four structures formed from corner-sharing tetrahedra are almost degenerate in energy and differ only for internal rotations giving different relative orientations to the two terminal AlCl_3 groups. However, of these the only mechanically stable structure at zero temperature is the C_2 one, which is obtained from a C_{2v} structure having an eclipsed arrangement of the terminal groups through opposite rotations of these groups by 30° around the $\text{Al}-\text{Cl}^B$ bond. The other structures have at least one imaginary

Table 4. Calculated equilibrium structure of the $(\text{Al}_2\text{Cl}_7)^-$, $(\text{Al}_2\text{Br}_7)^-$, $(\text{Ga}_2\text{Cl}_7)^-$ and $(\text{Ga}_2\text{Br}_7)^-$ anions in the C_2 configuration (the ranges of values shown for bond lengths and bond angles span those appropriate to inequivalent terminal halogens; the values for $(\text{Al}_2\text{Cl}_7)^-$ are from [7]. Bond lengths in Å and bond angles in degrees).

	$\text{M}-\text{X}^T$	$\text{M}-\text{X}^B$	$\angle \text{X}^T-\text{M}-\text{X}^T$	$\angle \text{X}^B-\text{M}-\text{X}^B$
$(\text{Al}_2\text{Cl}_7)^-$	2.10 - 2.12	2.35	100 - 108	111
$(\text{Al}_2\text{Br}_7)^-$	2.25 - 2.28	2.52	99 - 110	108
$(\text{Ga}_2\text{Cl}_7)^-$	2.16 - 2.18	2.40	100 - 107	111
$(\text{Ga}_2\text{Br}_7)^-$	2.30 - 2.33	2.56	99 - 109	108

mode frequency and therefore correspond to a multiplicity of saddle points separating several equivalent true minima. We may expect that at finite temperature the molecular ion will be executing rapid fluctuations between its various structures.

We have found that these structural properties hold for this anion in all other trihalides of present interest. Table 4 reports some of our results for equilibrium bond lengths and bond angles.

The same flexibility under rotations around the $\text{Al}-\text{Cl}^B$ bonds in chain-like structures is displayed by the $(\text{Al}_3\text{Cl}_{10})^-$ and $(\text{Ga}_3\text{Cl}_{10})^-$ trimeric anions. We find four structures for these anions, which are reported in Figure 1. All these chain-like structures are mechanically stable and differ very little in binding energy, at the level of hundredths of an eV. Again, rapid fluctuations in the hot melt are indicated.

The two structures of deepest energy are shown in Figs. 1.1 and 1.2. The trimer in Fig. 1.2 has a “stretched” configuration corresponding to the metal ions and bonding chlorines lying all in the same plane, while the structure in Fig. 1.1, which actually has a slightly deeper energy, is obtained from it by rotations of the terminal groups out of the plane. Relative to the values reported for the dimeric anions in Table 4, the bond lengths in these two structures of the trimeric anions are somewhat contracted in the central ionic group and somewhat expanded or (for the terminal chlorines) essentially unchanged in the external groups.

Figure 1.3 shows a “winged” structure for the trimeric anions, in which the bonds of the terminal metal ions to the bonding chlorines are twisted out of the plane. Finally, Fig. 1.4 shows a “cart” structure, in which the planar skeleton of the molecule is preserved but the central and terminal chlorines go into a staggered configuration. The “stretched”, “winged”, and “cart” structures for $(\text{Al}_3\text{Cl}_{10})^-$ have previously

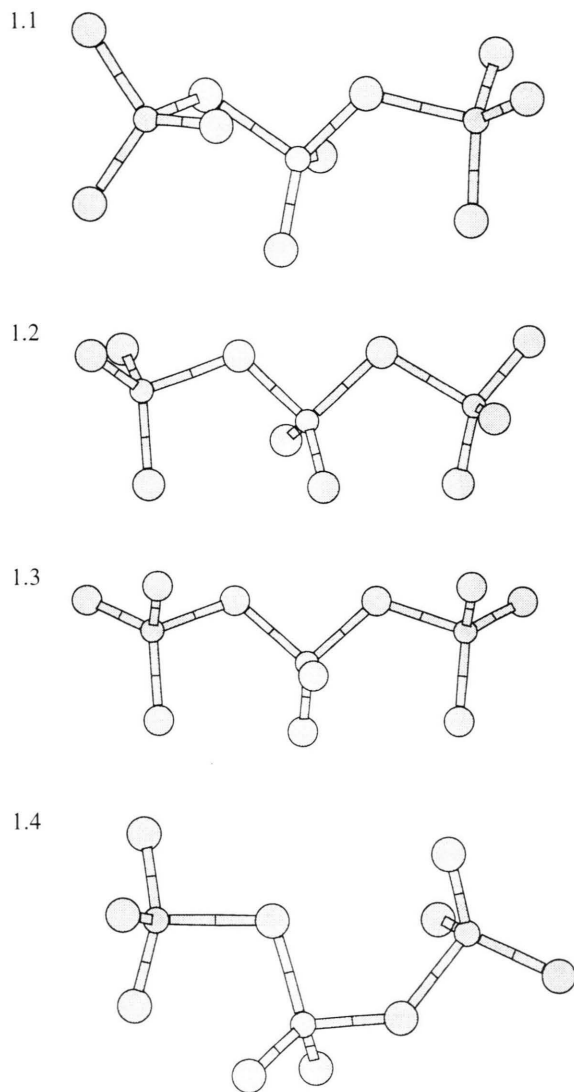


Fig. 1. Ball-and-stick models of four stable structures of the $(M_3Cl_{10})^-$ anion for $M = Al$ or Ga (see the discussion given in the text).

been reported from semi-empirical molecular orbital calculations by Dymek *et al.* [5].

Figure 2 shows a “stretched” chain-like configuration that we have found for the $(Al_4Cl_{13})^-$ and $(Ga_4Cl_{13})^-$ anion. All metal ions and bonding chlorines forming the backbone of the tetramer lie in a single plane. The bond lengths to the central bonding chlorine are 2.34 Å in $(Al_4Cl_{13})^-$ and 2.40 Å in $(Ga_4Cl_{13})^-$, *i. e.* practically the same as those reported in Table 4 for $(Al_2Cl_7)^-$ and $(Ga_2Cl_7)^-$. For the other

Table 5. Incremental binding energy $\Delta E^{(n)}$ of the $(Al_nCl_{3n+1})^-$ and $(Ga_nCl_{3n+1})^-$ series as a function of n (in eV).

	$n = 1$	$n = 2$	$n = 3$	$n = 4$
$(Al_nCl_{3n+1})^-$	2.29	0.76	0.61	0.49
$(Ga_nCl_{3n+1})^-$	2.18	0.78	0.61	0.53

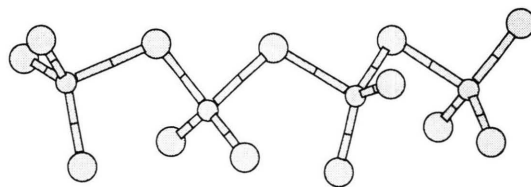


Fig. 2. A ball-and-stick model of the “stretched” structure of the $(M_4Cl_{13})^-$ anion for $M = Al$ or Ga .

bond lengths similar comments apply as those given above for $(Al_3Cl_{10})^-$ and $(Ga_3Cl_{10})^-$.

We conclude this section by reporting in Table 5 the increments $\Delta E^{(n)}$ in binding energy of the $(Al_nCl_{3n+1})^-$ and $(Ga_nCl_{3n+1})^-$ poly-anions on increasing n by unity in the range $1 \leq n \leq 4$. We have defined $\Delta E^{(n)} \equiv E_b^{(n)} - E_b^{(n-1)} - E_b(MCl_3)$, with $E_b^{(n)}$ the binding energy of the n -th member of the polymeric series and $E_b(MCl_3)$ the binding energy of MCl_3 . It is evident that the increase in binding energy of the two polymeric series on addition of an $AlCl_3$ or $GaCl_3$ group is converging quite rapidly to a constant amount of about 0.5 eV.

4. Energy Minima for Alkali Counterions

We report in this section our results on the potential energy minima of alkali counterions near dimeric anions, with main attention to the cases $A = Li, Na$ or K around an $(Al_2Cl_7)^-$ or an $(Al_2Br_7)^-$ anion. Similar results have been obtained for a Na counterion near $(Ga_2Cl_7)^-$ or $(Ga_2Br_7)^-$. The model parameters describing the overlap repulsion and the polarizability of alkali cations are as in earlier work on fluorides [17].

We find no qualitative dependence on the halogen, but a somewhat different structural behaviour for Li as opposed to Na and K . Figure 3 shows the deepest-energy configuration for Na or K around an $(Al_2X_7)^-$ anion. The alkali cation is coordinated by four of the terminal halogens, the bond length being 3.60 Å in the case of KAl_2Cl_7 . The corresponding $K-Cl^B$ distance is 4.99 Å and the $Al-Cl^B-Al$ bond angle is 115° . In semi-empirical molecular orbital calculations on AA_2Cl_7

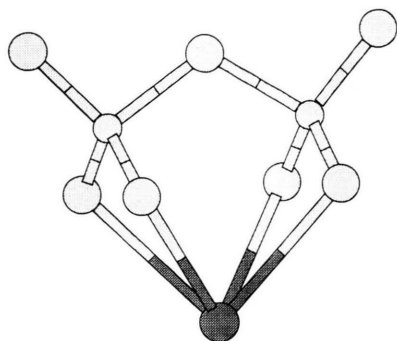


Fig. 3. A ball-and-stick model of the deepest-energy structure of the KA_2X_7 cluster for $\text{X} = \text{Cl}$ or Br . The K ion is shown as a dark sphere.

Blander *et al.* [3] reported a significant decrease of this bond angle on the approach of an alkali counterion, to a value of about 100° for K at a K-Cl^{B} distance of 5 Å. There is, therefore, disagreement in detail between our model and their results. However, from an X-ray diffraction experiment on KA_2Br_7 crystals Rytter *et al.* [18] reported an $\text{Al-Br}^{\text{B}}\text{-Al}$ bond angle of 109.3° and K-Br bond lengths in the range from 3.3 to 4.0 Å. Our corresponding results for the isolated KA_2Br_7 cluster are 112.6° and 3.74 Å.

Still considering the case of AA_2X_7 with $\text{A} = \text{Na}$ or K , we find two further distinct energy minima for the alkali counterion at a slightly higher energy than for the minimum shown in Figure 3. These minima correspond to (i) bonding of the counterion to the three terminal halogens in one of the AlX_3 groups, and (ii) bonding on top of the halogen bridge to the bridging halogen and to three further terminal halogens. It is evident from our calculations, therefore, that within our model the counterions are essentially free to move around the isolated poly-anion. This is consistent with essentially free migration of counterions in liquid mixtures.

As already noted, some details of the potential energy hypersurface for a Li counterion are somewhat different from the situation pertaining to Na and K . The smaller ionic size of Li tends to favour three-fold over fourfold coordination to the halogens, and in particular we find that the deeper energy minimum corresponds to binding to only three of the four bonding halogens shown in Figure 3. Again, free migration of the Li counterions is indicated.

5. Concluding Remarks

We have in this work determined a microscopic model of ionic interactions in aluminium and gallium trihalides and applied it to study the polymeric anion series which are formed in liquid Al -alkali and Ga -alkali halide mixtures. We have especially focused on the multiplicity of structures which are allowed for these chain-like anions by the considerable freedom of rotation of molecular groups around internal bonds and on the convergence of the value of the binding energy per monomer with increasing chain length. We have also examined the main features of the potential energy landscape for alkali counterions around dimeric anions.

The reasonable description afforded by our model for these complex ionic clusters suggests that it should find useful applications in further studies of these materials in the liquid state.

Acknowledgements

Three of us (Z. A., M. Ç., and Z. Ç.) acknowledge support received from the Turkish Scientific and Technological Research Council (Tubitak). Z. A. also acknowledges support from the Research Fund of the University of Istanbul under Project Number Ö-681/121099 and wishes to thank the Scuola Normale Superiore di Pisa for their hospitality during the final stages of this work.

- [1] Z. Akdeniz, D. L. Price, M.-L. Saboungi, and M. P. Tosi, *Plasmas and Ions* **1**, 3 (1998).
- [2] L. A. Curtiss, *Proc. Joint Int. Symp. Molten Salts*, ed. G. Mamantov; The Electrochemical Society, Pennington 1987, p. 185.
- [3] M. Blander, E. Bierwagen, K. G. Calkins, L. A. Curtiss, D. L. Price, and M.-L. Saboungi, *J. Chem. Phys.* **97**, 2733 (1992).
- [4] L. P. Davis, C. J. Dymek, J. J. P. Stewart, H. P. Clark, and W. J. Lauderdale, *J. Amer. Chem. Soc.* **1985**, 5041.
- [5] C. J. Dymek, J. S. Wilkes, M.-A. Einarsrud, and H. A. Øye, *Polyhedron* **7**, 1139 (1988).
- [6] K. R. Seddon, *Proc. Int. George Papatheodorou Symp.*, ed. S. Boghosian *et al.*; ICE/HT, Patras 1999, p. 131.
- [7] Z. Akdeniz and M. P. Tosi, *Z. Naturforsch.* **54a**, 180 (1999).
- [8] See e. g. R. A. Cochran, *Crit. Rev. Solid State Sci.* **2**, 1 (1971); J. R. Hardy and A. M. Karo, *The Lattice Dynamics and Statics of Alkali Halide Crystals*; Plenum Press, New York 1979.

- [9] M. P. Tosi and M. Doyama, *Phys. Rev.* **160**, 716 (1967).
- [10] P. Brumer and M. Karplus, *J. Chem. Phys.* **58**, 3903 (1973).
- [11] Wang Li and M. P. Tosi, *Nuovo Cim. D* **10**, 1497 (1988).
- [12] M. W. Chase, C. A. Davies, J. R. Downey, D. J. Frurip, R. A. McDonald, and A. N. Syverud, *J. Phys. Chem. Ref. Data* **14**, Suppl. No. 1 (1985).
- [13] Q. Shen, *Diss. Abstr. (Int.) B* **34**, 3735 (1974).
- [14] W. R. Busing, *Trans. Amer. Crystallogr. Assoc.* **6**, 57 (1970).
- [15] A. D. Alvarenga, M.-L. Saboungi, L. A. Curtiss, M. Grimsditch, and L. E. McNeil, *Molec. Phys.* **81**, 409 (1994).
- [16] S. Boghosian, D. A. Karydis, and G. A. Voyiatzis, *Polyhedron* **12**, 771 (1993).
- [17] Z. Akdeniz, Z. Çiçek, A. Karaman, G. Pastore, and M. P. Tosi, *Z. Naturforsch.* **54a**, 575 (1999).
- [18] E. Rytter, B. E. D. Rytter, H. A. Øye, and J. Krogh-Moe, *Acta Cryst. B* **29**, 1541 (1973).